REPORT DOCUMENTATION PAGE

Form Approved
OMB No. 0704-0188

1. REPORT DATE *(DD-MM-YYYY)*	2. REPORT TYPE	3. DATES COVERED *(From - To)*
	Final Report	1 January 2003 - 31 December 2005

4. TITLE AND SUBTITLE

Development of a Unified Code for Nonequilibrium Plasma Systems

5a. CONTRACT NUMBER

5b. GRANT NUMBER

F49620-03-1-0123

5c. PROGRAM ELEMENT NUMBER

6. AUTHOR(S)

Iain D. Boyd

5d. PROJECT NUMBER

5e. TASK NUMBER

5f. WORK UNIT NUMBER

7. PERFORMING ORGANIZATION NAME(S) AND ADDRESS(ES)

Department of Aerospace Engineering
University of Michigan
Ann Arbor MI 48109-2140

8. PERFORMING ORGANIZATION REPORT NUMBER

9. SPONSORING/MONITORING AGENCY NAME(S) AND ADDRESS(ES)

USAF/AFRL/NA
AFOSR
875 North Randolph Street
Arlington VA 22203
Dr John Schmisseur

10. SPONSOR/MONITOR'S ACRONYM(S)

AFOSR

11. SPONSOR/MONITOR'S REPORT NUMBER(S)

AFRL-SR-AR-TR-06-0135

12. DISTRIBUTION/AVAILABILITY STATEMENT

Distribution Statement A. Approved for public release; distributin is unlimited.

13. SUPPLEMENTARY NOTES

14. ABSTRACT

The goal of the project was to develop a new computational code to be used at the Arnold Engineering Development Center, (AEDC), Tullahoma, Tennessee, for analysis of plasmas characterized by high ionization fractions and extremely low number densities. Such conditions arise in two particular test facilities operated at AEDC: (1) the Decade Radiation Test Facility (DRTF), used to test the effects of strong radiation sources on materials and spacecraft components; and (2) the 12V Space Chamber, used to test electric propulsion (EP) thrusters used to control spacecraft. In order to have accurate predication of the quasi-neutral, kinetic flows in both facilities, the research was focused on developing a general, unsteady, electro-static, nonequilibrium gas and plasma simulation code that combined the capabilities of the direct simulation Monte Carlo (DSMC) method and the Particle-In-Cell (PIC) method. Efforts were also concentrated on applying the code to study the flows in the Decade and 12V facilities.

15. SUBJECT TERMS

16. SECURITY CLASSIFICATION OF:			17. LIMITATION OF ABSTRACT	18. NUMBER OF PAGES	19a. NAME OF RESPONSIBLE PERSON
a. REPORT	b. ABSTRACT	c. THIS PAGE			19b. TELEPHONE NUMBER *(Include area code)*
U	U	U	UU	21	

FINAL TECHNICAL REPORT

DEVELOPMENT OF A UNIFIED CODE FOR NONEQUILIBRIUM PLASMA SYSTEMS

AFOSR GRANT F49620-03-1-0123

Iain D. Boyd
Department of Aerospace Engineering
University of Michigan
Ann Arbor, MI 48109-2140

Abstract
The goal of the project was to develop a new computational code to be used at the Arnold Engineering Development Center, (AEDC), Tullahoma, Tennessee, for analysis of plasmas characterized by high ionization fractions and extremely low number densities. Such conditions arise in two particular test facilities operated at AEDC: (1) the Decade Radiation Test Facility (DRTF), used to test the effects of strong radiation sources on materials and spacecraft components; and (2) the 12V Space Chamber, used to test electric propulsion (EP) thrusters used to control spacecraft. In order to have accurate predication of the quasi-neutral, kinetic flows in both facilities, the research was focused on developing a general, unsteady, electro-static, nonequilibrium gas and plasma simulation code that combined the capabilities of the direct simulation Monte Carlo (DSMC) method and the Particle-In-Cell (PIC) method. Efforts were also concentrated on applying the code to study the flows in the Decade and 12V facilities.

Introduction
The objective of this project was to develop a new computational code to analyze the flows of plasmas characterized by high ionization fractions and extremely low number densities, for application to the Nuclear Weapons Effects (NWE) Decade facility and to the 12V Electric Propulsion (EP) plumes facility located at the Arnold Engineering Development Center (AEDC). Physically accurate numerical simulations are expected to play a significant role in optimizing the performance of the facilities as well as in playing an integral role in the testing capabilities provided by AEDC.

Typical flow conditions in Decade and 12 V give a Debye length and a mean free path that indicate that the flow is in the quasi-neutral, kinetic flow regime. Traditional continuum-based computational codes are unsuitable for very low density, or rarefied, gas and plasmas. Particle methods, such as the direct simulation Monte Carlo method (DSMC) [1], are becoming mature for modeling rarefied flows of neutral gases, but do not account for charged particle interactions. Particle-in-Cell (PIC) methods [2] account for field interaction effects of charged particles, but do not fully resolve particle energy and momentum transfer effects. Codes combining the capabilities of DSMC and PIC must be utilized to account for all the afore-mentioned effects in NWE and EP testing. This research effort will build upon existing DSMC and PIC techniques to develop a combined PIC/DSMC code directly applicable to AEDC's test facility needs: a general, unsteady, 3D, electro-static nonequilibrium gas and plasma simulation code that is readily usable by engineers at AEDC for analysis of the Decade and 12V facilities.

Accomplishments
Starting with an existing, general, 3D DSMC code called MONACO, we added many new capabilities required to accurately model the AEDC facility flows, performed solid code validations, and studied typical flows experienced in the Decade and 12V facilities.

Code Development
We have added many features to MONACO that expands the capability of the code and improves the interface to users. Motivated by the Decade unsteady flows, we added the following features:

- The ability to routinely run unsteady simulations.
- The ability to accept multiple flow boundary conditions.
- The ability to set multiple initial flow conditions.
- The subcell technique for collision pair selection [1].

- The near-partner technique for collision pair selection [3].
- The ability to perform dynamic domain decomposition for the unsteady flows executed on parallel computers by integrating Metis package [4].
- The relaxation technique to estimate macroscopic flow properties [5].
- Feedback to users on simulation parameters.
- A utility to generate particle weight of cells.

Many of these features improve the generality or efficiency of the code. For instance, the subcell selection technique allows the cell size of the grid to be larger than the mean free path of molecules, thus avoids a new simulation using a finer grid. The parallel domain decomposition technique enables the workloads to be equally distributed on all processors, which can improve the parallel efficiency by several times. The code has been widely validated and the results agree very well with published data. The validation ranges from one-dimensional to three-dimensional flows, and includes subsonic and supersonic flows. In addition, work this year focused on the development of a new condensation model that is consistent with the DSMC technique [6]. This modeling was found to be required due to the very low temperatures experienced in DECADE, and is described in detail below.

The 12V flows involve plasma jet expansions from an electric propulsion device into the vacuum chamber. Thus far, for these flows, we have added the following capabilities to MONACO:

- The ability to simulate electro-static plasma using the Particle-In-Cell (PIC) method. The ions are treated as particles and the electrons as a fluid.
- The general unstructured grid implementation for the PIC method.
- The important collision mechanism of charge exchange.
- Particle weighting by species.
- New diagnostics (e.g., ion energy distribution).

More technical details are provided in the later portions of this report.

Transitions

Updated version of MONACO software delivered to Ken Tatum, Aerospace Testing Alliance, Arnold AFB.

Acknowledgment / Disclaimer

This work was sponsored by the Air Force Office of Scientific Research, USAF, under AFOSR Grant F49620-03-1-0123. The views and conclusions contained herein are those of the author and should not be interpreted as necessarily representing the official policies or endorsements, either expressed or implied, of the Air Force Office of Scientific Research or the U.S. Government.

References

[1] Bird, G.A., *Molecular Gas Dynamics and the Direct Simulation of Gas Flows,* Oxford University Press, 1994.

[2] Birdsall, C.K. and Langdon, A.B., *Plasma Physics Via Computer Simulation*, Hilger, 1991.

[3] Sun, Q., Cai, C., Boyd, I.D., Clemmons, J.H., and Hecht, J.H., "Analysis of High-Altitude Ionization Gauge Measurements Using the Direct Simulation Monte Carlo Method," AIAA-04-2686, June 2004.

[4] Karypis, G. and Kumar, V., "METIS, A Software Package for Partitioning Unstructured Graphs, Partitioning Meshes, and Computing Fill-Reducing Orderings of Sparse Matrices, version 4.0," Technical Report, University of Minnesota, 1998.

[5] Sun, Q. and Boyd, I.D., "Evaluation of Macroscopic Properties in the Direct Simulation Monte Carlo Method," *Journal of Thermophysics and Heat Transfer*, Vol. 19, 2005, pp. 329-335.

[6] Sun, Q., and Boyd, I.D., "Modeling Gas Nucleation and Condensation Using the Direct Simulation Monte Carlo Method," AIAA-2005-4831, June 2005.

Publications

(1) Sun, Q., and Boyd, I.D., "Modeling Gas Nucleation and Condensation Using the Direct Simulation Monte Carlo Method," AIAA-2005-4831, June 2005.

(2) Boyd, I.D., Sun, Q., Cai, C., and Tatum, K.E., "Particle Simulation of Hall Thruster Plumes in the 12V Vacuum Chamber," IEPC-05-138, October 2005.

(3) Sun, Q. and Boyd, I.D., "Evaluation of Macroscopic Properties in the Direct Simulation Monte Carlo Method," *Journal of Thermophysics and Heat Transfer*, Vol. 19, 2005, pp. 329-335.

TECHNICAL DETAILS

1. Decade Flow Investigations

In recent years there has been much interest in the behavior of clusters. The formation and growth of clusters through gas nucleation and condensation is believed essential to many phenomena. For instance, vapor-liquid nucleation processes play an important role in the formation of atmospheric aerosols.[1] The formation of soot begins with formation of clusters.[2] Gas condensation can also occur within thruster plumes, and clusters may cause contamination of the rocket surfaces.[3] The formation of clusters will affect the supersonic flow in expansion nozzles due to the heat released during the phase change process.[4] Cluster formation and growth is also involved in many material processes, including chemical vapor deposition,[5] dry etching,[6] and nanoscale material manufacturing.[7] Understanding the mechanism of the gas nucleation (cluster formation) and condensation (cluster growth) will therefore help improve fabricating techniques and the quality of the resultant products.

Studies on gas nucleation and condensation are generally based on two approaches: continuum approach and kinetic approach. The continuum approach is usually called classical nucleation theory[8,9] that is derived from thermodynamics. It is assumed that homogeneous nucleation starts when the free energy loss from the transition of gas molecules into the liquid phase can compensate for the energy increase resulting from the surface tension of a cluster. Different expressions have been derived for the nucleation rate, and some of them can differ by a factor of 10^{17} for the magnitude of the nucleation rate.[9] Furthermore, the surface tension of clusters is still unclear yet. If the value of the bulk material is used for the surface tension of clusters, an advanced expression (Lothe and Pound[10]) for the nucleation rate predicts a much worse nucleation rate than a simple expression (Becker and Doring[8]) as compared with measurement data. Therefore there are still many uncertainties in the classical nucleation theory. On the other hand, many efforts have been made recently to develop kinetic approaches. One is called Smoluchowski's approach where nucleation is viewed as a process of chemical aggregation.[11] The key issue is to determine the rate constants that are still unresolved yet. A fundamental approach for studying nucleation and condensation is the molecular dynamics method that simulates molecular movement and interactions directly.[12] This approach is supposed to expose the detailed nucleation and condensation processes, and has been applied to study gas nucleation and condensation.[8,13-16] However, studies using molecular dynamics are limited to systems with few clusters or/and clusters having small size because of the large numerical cost for simulations. It is impractical to simulate meso-scale systems such as supersonic flow in an expansion nozzle based on the current computational capability.

A more efficient kinetic approach, the direct simulation Monte Carlo (DSMC) method,[17] has been introduced into the field of gas nucleation and condensation. The DSMC method is less numerically expensive than molecular dynamics but still kinetically accurate, and gas nucleation and condensation models can be easily implemented in the DSMC method. Therefore, the DSMC method is becoming a popular approach for model testing and flow investigation.[11,18-22] For instance, Hettema and McFeaters[11] used the DSMC method to implement the Smoluchowski approach; Zhong et al.[21] employed the classical nucleation theory in the DSMC method studying supersonic plumes. Most of these applications, however, have neglected the cluster effects on gas flows, which then affects the cluster modeling. There are two significant influences of clustering on gas flows: the removal of a portion of the vapor phase and the "heating" of the remainder to absorb the energy extracted from the condensed phase. In the usual case, the ratio h_{fg}/C_pT (h_{fg} being the enthalpy change during condensation, C_p being the specific heat, and T is the local temperature) is greater than unity and this means that "heating" has a larger effect on the stream properties than the vapor removal.[4] These effects were partially demonstrated in the plume studies by Perrell et al. although a continuum-based approach was used.[23] We also showed the clustering effects on gas flow in our previous paper when studying gas expansion in a supersonic nozzle by including dimers in the simulation.[22] However, there is no systematic nucleation and condensation model developed for the DSMC method yet.

The main goal of this study is to develop a general nucleation and condensation model to be implemented in the DSMC method. The model itself is not able to predict the value of parameters for simulations, but is supposed to utilize new results from molecular dynamics simulations. The rest of the paper is organized as follows. Brief description of homogeneous nucleation and condensation theory is given in section II. Then microscopic modeling that is suitable for the DMSC method is discussed in section III. Several parametric studies are given in section IV. Finally, the paper ends with some concluding remarks.

Homogeneous Nucleation and Condensation Theory

A gas is regarded as undersaturated, saturated, or supersaturated if the pressure of the gas (P) is less than, equal to, or larger than the equilibrium saturation value (P_s) corresponding to the local temperature. The undersaturated and saturated states are thermodynamically stable, whereas the supersaturated state is unstable. The supersaturated gas will nucleate and condense in the presence of impurities or walls. Otherwise, the gas sustains a very high degree of saturation ($S = P/P_s$) until homogeneous nucleation occurs.

There are generally two different views on the homogeneous nucleation processes. The classical nucleation theory (CNT) indicates that nucleation begins after the "energy barrier" is overcome; whereas kinetic approaches, such as Smoluchowski's approach, assume that nucleation starts from formation of dimers. In the classical nucleation theory, it is assumed that clusters grow or shrink via the attachment or loss of a single molecule. Making this approximation leads to a set of coupled rate equations for the number density of clusters of different size. Further with the equilibrium state assumption, the nucleation rate (J) can be expressed as follows:

$$J = \frac{cP\left(4\pi r_*^2\right)n}{\sqrt{2\pi mkT}} \exp\left(-\frac{\Delta G^*}{kT}\right) \tag{1}$$

where r_* is the critical cluster radius, and ΔG^* is the free energy of formation of a critical-sized cluster. The other variables are: Boltzmann constant k, gas number density n, molecular mass m, and constant c. The critical size is defined such that the free energy of formation reaches the maximum value at this size, and clusters larger than this size are stable whereas smaller clusters are thermodynamically unstable. The CNT relies on a macroscopic approximation for evaluation of the free energy of clusters. This of course makes no sense for small clusters of a few molecules. There are also arguments on the number of degrees of freedom to be included in the evaluation of free energy.[9] In general, the nucleation rate can be expressed using a nucleation constant (c_n):

$$J = c_n \sqrt{\frac{2\sigma}{\pi m^3}} \frac{\rho_v^2}{\rho_l} \exp\left(-\frac{4\pi r_*^2 \sigma}{3kT}\right) \tag{2}$$

where σ is the surface tension of clusters, and ρ_l, ρ_v are the mass densities of liquid and vapor, respectively. The critical cluster radius is given as

$$r_* = \frac{2\sigma}{\rho_l RT \ln S} \tag{3}$$

Determining the value of σ is another challenge. There is no general agreement on how the surface tension relates to the radius of curvature.[4] The surface tension is also temperature-dependent. Although there are several uncertainties in the CNT, measurement data can actually follow the CNT prediction (expression (2)) for most cases.[8] However, when the vapor temperature is low, the critical size predicted by CNT may not be reasonable. For instance, for condensation of water vapor in air at low temperatures $T < 270K$, the size of the critical cluster determined by CNT is less than the water molecule itself.[24] Some even suggested not to use the CNT for modeling the onset of clustering in supersonic beams.[25]

Kinetic approaches, however, do not use the concept of "equilibrium state" and there is no critical cluster size. Clusters are formed when two molecules approach each other and form a bound state. It is generally assumed that the formation of a bound state is feasible only when a third particle interacts with one of the two particles and carries away the kinetic energy. Molecular dynamics simulation by Zeifman et al. confirmed that condensation starts from dimer formation in triple collisions of monomers.[26] The nucleation rate, however, has not been generally determined. Because clusters can dissociate, the cluster distribution can diverge as the volume containing the clusters increases. Treatment of the volume dependence of the free energy has been a source of confusion and controversy in the development of a general molecular theory of nucleation. Other kinetic approaches, however, cannot predict the nucleation rate. For instance, the Smoluchowski approach treats cluster formation as a chemical reaction, but the value of rate constants is unavailable from the approach itself. Another difference is that a third particle is not included for the cluster formation reaction in the Smoluchowski approach. Overall, there is no general expression for the nucleation rate in kinetic approaches.

There are fewer discrepancies about the growth and depletion of clusters. Both continuum and kinetic approaches assume that cluster condensation and evaporation proceeds via one monomer at a time. Other

processes such as re-arrangement and fragmentation processes are sometimes included. When a monomer has a collision with a cluster, a sticking coefficient (q_s) is used to indicate the possibility for a condensation event. Then the condensation mass flux can be expressed as $q_s P/\sqrt{2\pi RT}$. A collision between a monomer and a cluster can also activate the cluster to evaporate. The evaporation mass flux is derived such that the evaporation mass flux is equal to the condensation mass flux in equilibrium, and is expressed as $q_s P_d/\sqrt{2\pi RT_d}$, where T_d is the cluster temperature and P_d is the hypothetical ambient pressure which would be necessary to keep the cluster in equilibrium.

Microscopic Modeling

Gas nucleation and condensation are essentially kinetic processes. Detailed description of these processes, however, is numerically too expensive; and it is unnecessary for many practical applications. A statistical description is then more useful for numerical simulations. In this section, we will discuss some properties of clusters, and develop microscopic models that can be easily implemented in the direct simulation Monte Carlo method for gas nucleation and condensation.

Some Properties of Clusters

Theoretically, clusters bridge the gap between microscopic gas and macroscopic materials. The behavior of small clusters (dimer, trimer, etc.) is governed by atomic and molecular mechanics whereas the behavior of large-sized clusters is governed by the macroscopic properties of the material. Therefore, as clusters form and grow, their behavior develops from the molecular to the bulk behavior.

Clusters are treated as particles so that microscopic behavior of clusters can be well represented. For simplicity, only a monatomic gas is discussed in this study. If we denote a j-mer as a cluster having j atoms, then the mass of a j-mer is jm. Its translational energy (E_{TE}) is $jmV_j^2/2$, where V_j is the translational speed of the j-mer. The average of the translational energy is then $3kT_j/2$ from gas kinetic theory, where T_j is the temperature of the j-mer. The internal energy (E_{IE}) of a j-mer is assumed to have an average of $3(j-1)kT_j/2$ so that the total of the translational energy and internal energy of a j-mer is equal to the corresponding total of j atoms. Unlike gas atoms, clusters have potential energy (E_{PE}), which can be expressed as $-jh_{fg}(T_j, j)$. Here, $h_{fg}(T_j, j)$ is the latent heat of evaporation of the cluster. Clearly, $h_{fg}(T_j, j)$ should be small for small clusters because there are relatively few bonds for each atom; and it should approach the latent heat of evaporation of liquid ($h_{fg}(T_j)$) when the cluster size increases. The latent heat of evaporation is temperature-dependent, and its relation can be derived using the first law of thermodynamics:

$$E_{TE} + E_{IE} + E_{PE} + Q = E_{TE0} + E_{IE0} + E_{PE0} \tag{4}$$

$$\frac{3}{2}kT + \frac{3}{2}(j-1)kT - jh_{fg}(T) + jC_p k(T_0 - T) = \frac{3}{2}kT_0 + \frac{3}{2}(j-1)kT_0 - jh_{fg}(T_0) \tag{5}$$

$$h_{fg}(T) = \left(C_h - \frac{3}{2}\right)k(T_0 - T) + h_{fg}(T_0) \tag{6}$$

where Q is the heat required to heat the cluster from T to T_0. The dependence of the latent heat on cluster size is still unclear. If we refer to the often used binding energy expression $E_b(j) = a_v j + a_s j^{2/3}$ (a_v and a_s are constants corresponding to the volume and surface terms),[19] the latent heat of evaporation of clusters is assumed as follows:

$$E_{PE}(T, j) = -jh_{fg}(T)\left(1 - C_a j^{-1/3} + C_b j^{-1}\right) \tag{7}$$

where the last term is added to increase options for parametric studies. If clusters are assumed as spheres, the radius is therefore $j^{1/3} r_1$ based on the volume. In fact, the radius of clusters is better represented by

$$r_j = A j^{1/3} + B \tag{8}$$

as predicted by molecular dynamics simulation,[27] where A and B are constants. Molecular dynamics simulations also show that the cluster radius depends on the relative collision velocity as in the variable hard sphere molecular model:[17]

$$r = r_{ref}\left(\frac{V_{ref}}{V_r}\right)^{\nu} \tag{9}$$

where ν is the temperature index of the viscosity, which also depends on the cluster size.[27]

Nucleation

As discussed in Section II, there is no general kinetic expression for gas nucleation. The expression from the classical nucleation theory is then used to derive a microscopic expression for the nucleation rate. A multiplicative factor may be used in the expression, and parametric studies may be performed to study effects of this factor. Here, we assume that the formation of dimers is the onset of nucleation as in general kinetic approaches. For simplicity, the third particle is also omitted and the metastable collision complex is assumed stabilized upon the next collision. This assumption is acceptable since we do not really know what the value of the nucleation rate is. The nucleation rate is then converted to a nucleation probability of binary collisions. Namely, a nucleation event occurs according to the probability of nucleation, which is derived as follows:

$$P_N = \frac{C_n\sqrt{8m\sigma/\pi}}{\rho_l(\sigma_T V_r)}\exp\left(-\frac{4\pi r_*^2\sigma}{3kT}\right) \tag{10}$$

where σ_T is the collision cross section.

After a nucleation event occurs, the status of the formed dimer can be evaluated as follows:

$$mV_1 + mV_{1'} = 2mV_2 \tag{11}$$

$$\frac{1}{2}mV_1^2 + \frac{1}{2}mV_{1'}^2 = \frac{1}{2}2mV_2^2 + \frac{3}{2}kT_2 + E_{PE}(T_2,2) \tag{12}$$

then

$$V_2 = \frac{1}{2}(V_1 + V_{1'}),\ \frac{3}{2}kT_2 = \frac{m}{4}V_r^2 - E_{PE}(T_2,2) \tag{13}$$

Condensation and Evaporation

When a monomer collides with a cluster, there are three possible collision types: condensation, evaporation, and regular reflection. We combine the condensation and evaporation probabilities into one probability, and use the sign of the combined probability to indicate a possible nucleation or condensation event. The combined condensation- evaporation probability is derived as:

$$p_c = q_s - q_s\frac{p_d}{p}\sqrt{\frac{T}{T_d}} \tag{14}$$

Here a positive value of p_c indicates condensation, and a negative value refers to evaporation. If neither condensation nor evaporation occurs, the monomer-cluster collision is a scattering collision where full thermal accommodation is typically assumed. The status of particles after collisions are derived as follows:

Condensation

$$mV_1 + jmV_j = (j+1)mV_{j+1} \tag{15}$$

$$\frac{1}{2}mV_1^2 + \frac{1}{2}jmV_j^2 + \frac{3}{2}(j-1)kT_j + E_{PE}(T_j,j) = \frac{1}{2}(j+1)mV_{j+1}^2 + \frac{3}{2}jkT_{j+1} + E_{PE}(T_{j+1},j+1) \tag{16}$$

then

$$V_{j+1} = \frac{1}{j+1}(V_1 + jV_j) \tag{17}$$

$$T_{j+1} = \frac{\left(\frac{3}{2}(j-1)+\left(C_r-\frac{3}{2}\right)\left(j-C_v j^{2/3}+C_v\right)\right)kT_j + \frac{1}{2}\frac{j}{j+1}mV_r^2 + \left(\left(C_r-\frac{3}{2}\right)kT_0 + h_R(T_0)\right)\left(1+C_v\left(j^{2/3}-(j+1)^{2/3}\right)\right)}{\frac{3}{2}jk + \left(C_r-\frac{3}{2}\right)k\left(j+1-C_v(j+1)^{2/3}+C_v\right)} \tag{18}$$

Evaporation

$$V_c = V_{j+1} \tag{19}$$

$$\begin{cases} \frac{1}{2}\frac{j}{j+1}mV_r^2+\left(\frac{3}{2}(j-1)+\left(C_p-\frac{3}{2}\right)\left(j-C_a j^{2/3}+C_b\right)\right)kT_j \\ \quad =\left(\frac{3}{2}jk+\left(C_p-\frac{3}{2}\right)k\left(j+1-C_a(j+1)^{2/3}+C_b\right)\right)T_{j+1}-\left(\left(C_p-\frac{3}{2}\right)kT_0+h_{fk}(T_0)\right)\left(1+C_a\left(j^{2/3}-(j+1)^{2/3}\right)\right) \quad j>1 \\ \frac{1}{2}\frac{1}{2}mV_r^2=\frac{3}{2}kT_2+E_{PE}(T_2,2) \quad j=1 \end{cases} \tag{20}$$

Reflection

$$V_c=\frac{1}{j+1}\left(V_1+jV_j\right) \tag{21}$$

$$\frac{1}{2}\frac{j}{j+1}mV_r'^2+\left(\frac{3}{2}(j-1)+\left(C_p-\frac{3}{2}\right)\left(j-C_a j^{2/3}+C_b\right)\right)kT_j'=\frac{1}{2}\frac{j}{j+1}mV_r^2+\left(\frac{3}{2}(j-1)+\left(C_p-\frac{3}{2}\right)\left(j-C_a j^{2/3}+C_b\right)\right)kT_j \tag{22}$$

Note that the post-collision status is determined only for a condensation event. The status for an evaporation or reflection event is not determined. A general procedure for this undetermined status is to use the Borgnakke-Larsen model,[17] which is explained in the next sub-section.

Larsen-Borgnakke Model

The Larsen-Borgnakke model is widely used in the DSMC method to redistribute total collision energy between translational and internal energy modes by sampling energy from two equilibrium distributions. Using the equal- partition principle, the distribution of energy E_a from a total of E_a+E_b can be expressed as follows:

$$f(x)=f\left(\frac{E_a}{E_a+E_b}\right)=\frac{\Gamma(\xi_a+\xi_b)}{\Gamma(\xi_a)\Gamma(\xi_b)}x^{\xi_a-1}(1-x)^{\xi_b-1} \tag{23}$$

where ξ_a and ξ_b are the numbers of degrees of freedom for E_a and E_b, respectively. The instant value of energy E_a is sampled using the acceptance-rejection method.[17] Namely, a value of E_a is chosen randomly between zero and E_a+E_b, then this value is used to calculate its probability ratio using Eq. (24) and is compared with a random

$$\frac{P}{P_{\max}}(x)=\left(\frac{\xi_a+\xi_b-2}{\xi_a-1}x\right)^{\xi_a-1}\left(\frac{\xi_a+\xi_b-2}{\xi_b-1}(1-x)\right)^{\xi_b-1} \tag{24}$$

fraction R_f that is generated from a uniform distribution between 0 and 1. This value of E_a is accepted if the probability ratio is greater than R_f, but a new value is chosen and the process is repeated if the ratio is less than R_f. However, when ξ_a and ξ_b are not of the same order of magnitude, many attempts have to be made to find a value of E_a. A remedy is to avoid finding x itself by converting x to a new variable y whose value is close to 0.5 by using a transformation $y=x^{1/a}$. The value of a can be chosen as $\log_2^{(\xi_a+\xi_b)/\xi_a}$. Then the distribution for y is

$$f(y)=\frac{a\Gamma(\xi_a+\xi_b)}{\Gamma(\xi_a)\Gamma(\xi_b)}\left(y^a\right)^{\xi_a-1/a}\left(1-y^a\right)^{\xi_b-1} \tag{25}$$

and the probability ratio is

$$\frac{P}{P_{\max}}(y)=\left(\frac{\xi_a+\xi_b-1-1/a}{\xi_a-1/a}y^a\right)^{\xi_a-1/a}\left(\frac{\xi_a+\xi_b-1-1/a}{\xi_b-1}\left(1-y^a\right)\right)^{\xi_b-1} \tag{26}$$

To compare the numerical performance of the standard and modified Larsen-Borgnakke models, the average number of attempts required during the acceptance-rejection procedure is plotted in Fig. 1 (a) where the percentage of one

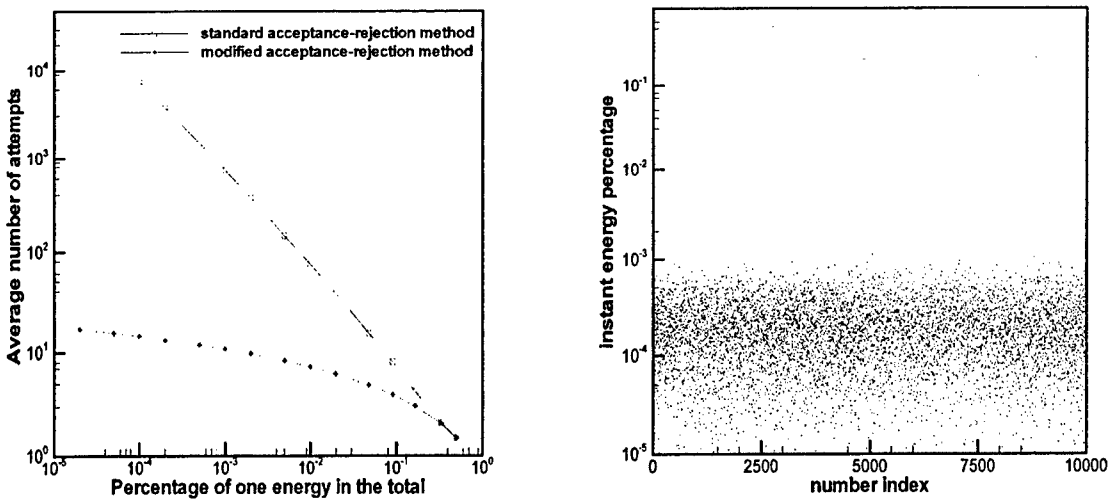

(a) (b)

Figure 1. Numerical performance of the Larsen-Borgnakke model. *(a) comparison of number of attempts during the acceptance-rejection procedure, (b) instant distribution of the energy percentage using the standard Larsen-Borgnakke method.*

energy in the total is $E_a/(E_a+E_b)$. Clearly, the modified Larsen-Borgnakke method improves greatly the numerical efficiency when ξ_a is much smaller than ξ_b, which is usually the case for clusters having many atoms. Numerical tests also show that the standard Larsen-Borgnakke method can accept unusual values with a relatively large probability. For example, Fig 1(b) shows the instant energy percentage ($E_a/(E_a+E_b)$) distribution whose theoretical average value is $2e^{-4}$. We find that there are 4 values larger than 0.1 among 10,000 values, which is statistically too much. These undesired values, however, are avoided when the modified Larsen-Borgnakke method is employed (the plot is otherwise similar to Fig. 1(b), and is therefore not shown).

Parametric Studies

The developed kinetic model is implemented in the DSMC research code "MONACO".[28] The clusters are modeled as particles in a similar way to monomers. Clusters have translational velocity; and their internal and potential energy is represented by the cluster temperature. The sub-relaxation technique[29] is employed to evaluate the macroscopic properties (gas temperature, pressure, et al.) that are explicitly involved in the developed microscopic model. We use argon gas to illustrate the nucleation and condensation processes.

As discussed in Section III, there are many uncertainties about the nucleation and condensation processes. For simplicity, the clusters are modeled as hard spheres, which means that the cluster radius is calculated as $j^{1/3}r_1$. The surface tension of clusters is approximated as $0.0344(1-T/T_c)$ N/m following Hale,[30] where the critical temperature (T_c) is about 150.85K. The saturated vapor pressure P_s is used as P_d for the evaporation calculation. The saturated vapor pressure is written using a logarithmic-exponential curve-fit expression as follows:

$$\ln P_s = -396.465 + 225.279 \ln T - 41.7722 \ln^2 T + 2.6374 \ln^3 T \qquad (27)$$

when the temperature is in the range between 20K and 150.85K.

Two numerical examples are employed to study effects of several parameters on gas nucleation and condensation. One is a box flow. The argon gas represented by 90,000 particles is simulated in a square box where the box surface is assumed specular. The initial number density and temperature are $1\times10^{26}/m^3$ and 55K, respectively. Other parameters are set as following unless specified otherwise: $C_n = 10^8$, $q_s = 0.1$, $C_a = 2.0$, and $C_b = 1.175$. The second example involves supersonic flow in an expansion nozzle.

Nucleation Rate

There is not much information about the nucleation rate at low temperature. It is therefore very important to study effects of this rate on flow properties. Figure 2 shows some plots using three different values for the rate constant. In this study, evaporation of a dimer to two monomers is disabled because fluctuation of flow properties cannot nucleate a dimer after a dimer is accidentally evaporated. These plots show that the number of clusters increases linearly at the early time and then quickly reaches a constant as the degree of supersaturation decreases because the monomers are converted into clusters and gas temperature is increased. The average cluster size is almost independent of the nucleation rate at very early time, but then increases in a behavior dominated by the condensation process (smaller nucleation rate corresponds to larger clusters). Both gas and cluster temperatures increase as more and more gas is converted into clusters, and the gas temperature lags behind the cluster temperature. It takes more than a tenth of a microsecond to reach the steady state. In general, a larger nucleation rate means that there will be more clusters but having a smaller average size, and the gas will be heated quicker but there is less effect on the final flow temperature which is basically determined by the vapor pressure.

Sticking Coefficient

The sticking coefficient is usually pre-assumed for condensation simulations. Recent studies of Zhong et al.[27] showed that the sticking coefficient depended on the cluster size. For the time being, we only consider a fixed sticking coefficient for all clusters. Figure 3 shows comparisons of several flow properties using three different values for the sticking coefficient. Clearly, the sticking coefficient has no effect on the number of clusters at early time, but a larger sticking coefficient means a large cluster size and later limits the number of clusters at steady state. Because the sticking coefficient determines the condensation rate, it also affects the temperature of both gas and clusters. A larger sticking coefficient will heat the gas more quickly. If the sticking coefficient is very small, then gas-cluster collisions will have a larger possibility for a reflection collision; so the gas temperature can closely follow the cluster temperature.

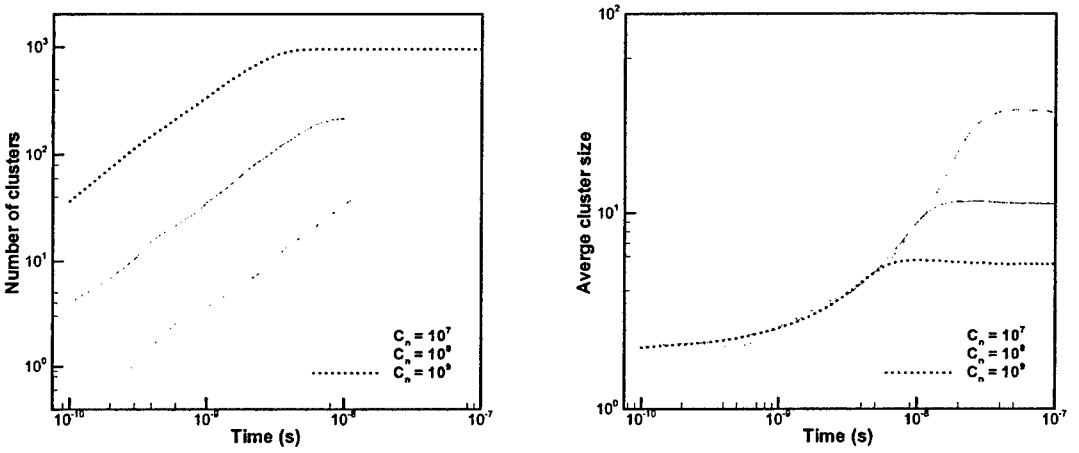

(a) (b)

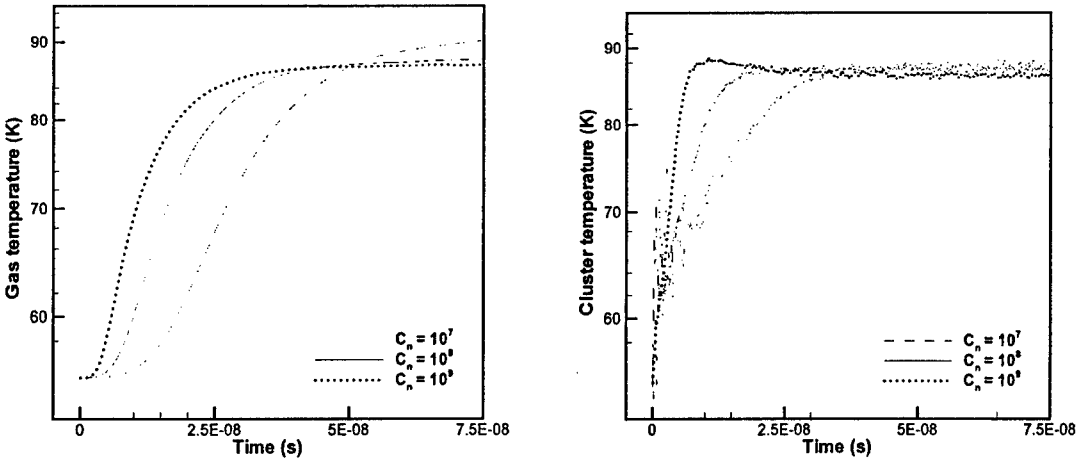

(c) (d)

Figure 2. Effects of nucleation rate on flow properties. *(a) number of clusters, (b) average cluster size, (c) gas temperature, (d) cluster temperature.*

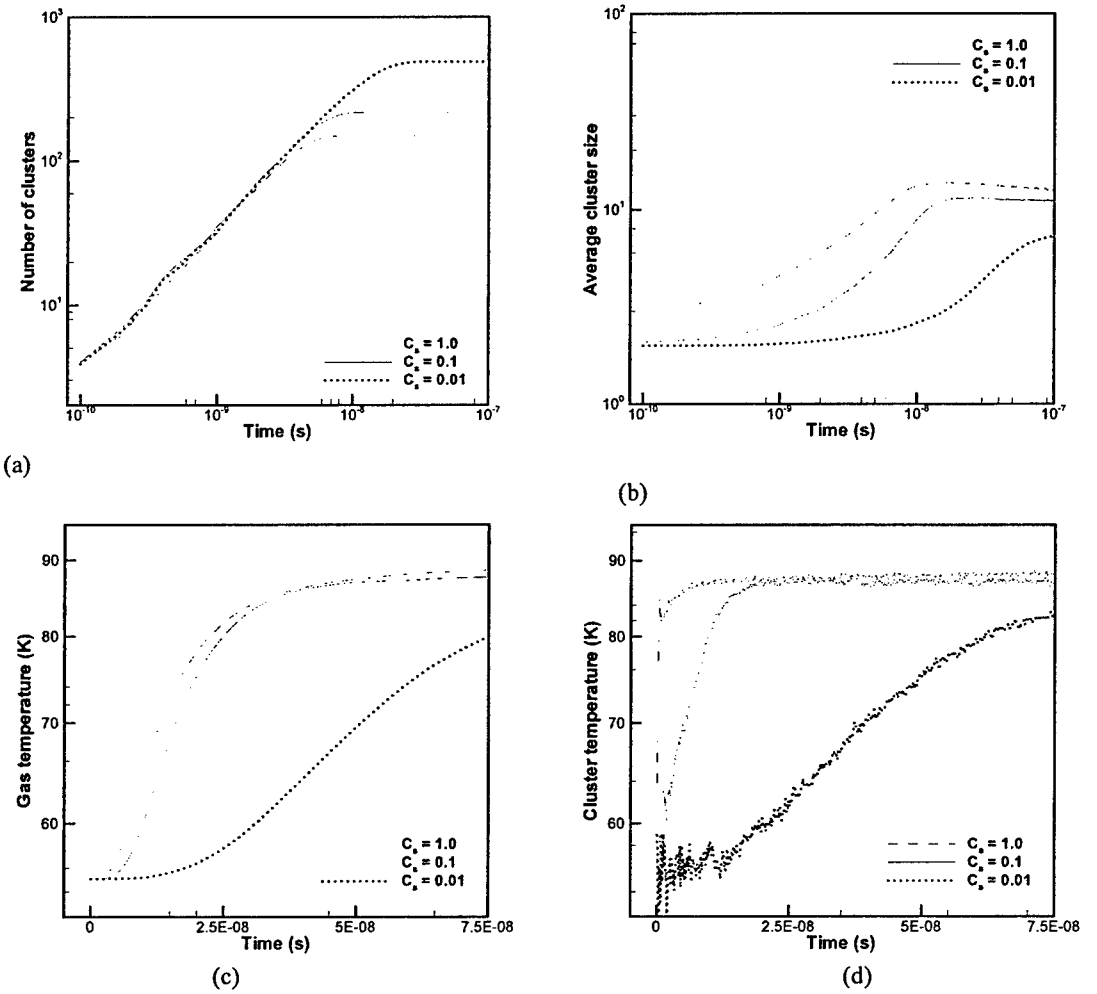

(a) (b)

(c) (d)

Figure 3. Effects of sticking coefficient on flow properties. *(a) number of clusters, (b) average cluster size, (c) gas temperature, (d) cluster temperature.*

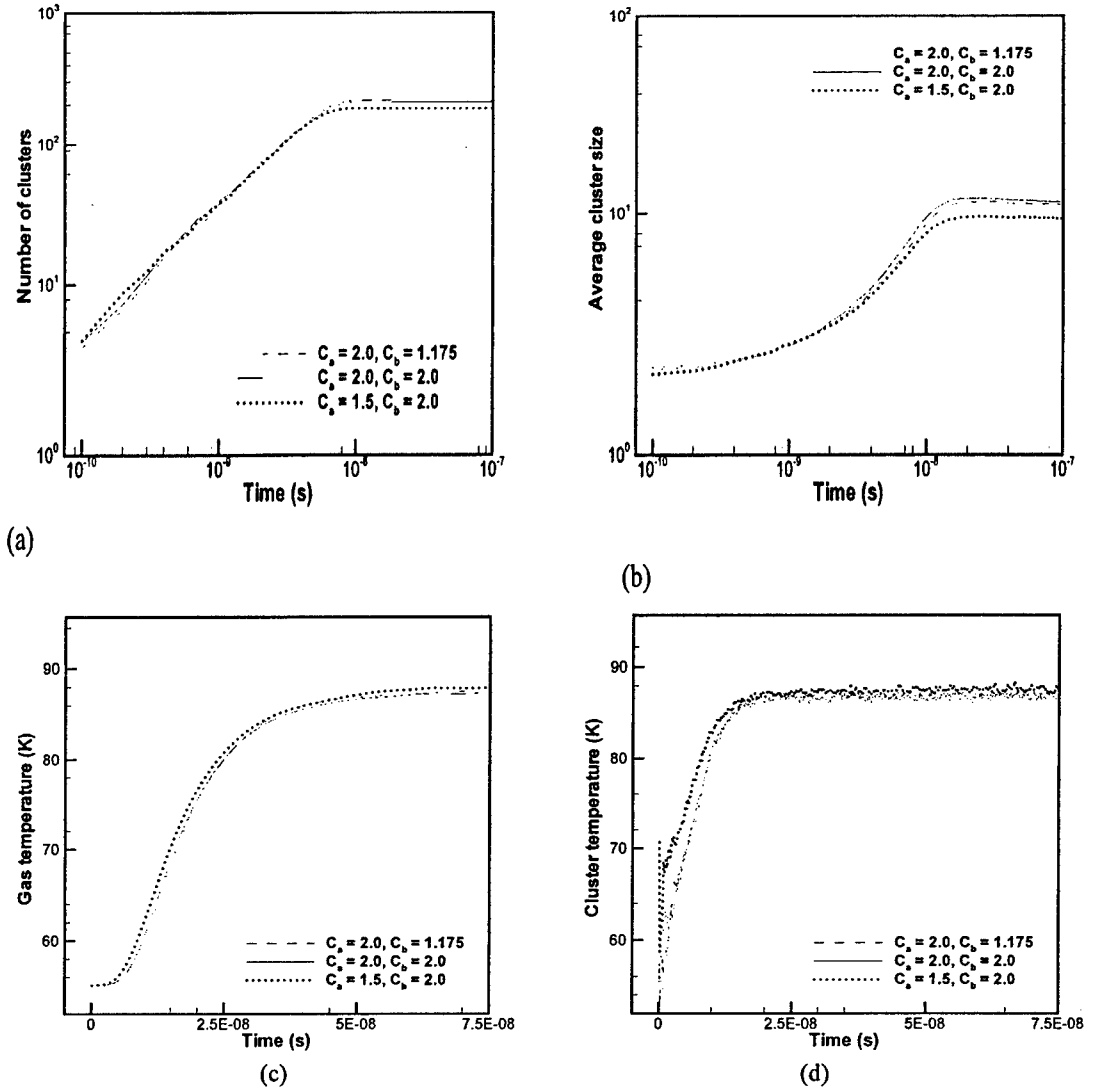

Figure 4. Effects of potential energy on flow properties. *(a) number of clusters, (b) average cluster size, (c) gas temperature, (d) cluster temperature.*

Potential Energy

The value of potential energy is also unclear for small clusters. We therefore test effects of potential energy on flow properties. Figure 4 shows some results using several different values for the potential energy. Maybe because of the small sticking coefficient (0.1), there are no large effects of the potential energy tested on the flow properties. Further studies are required to draw solid conclusions for effects of the potential energy.

Supersonic Flow in Expansion Nozzle

It is not unusual that gas nucleation and condensation occurs in supersonic flow in expansion nozzles.[4,21-22] We use a simple example to illustrate the gas nucleation and condensation phenomena in supersonic expansion flows. The expansion nozzle is two dimensional, and the surface is assumed specular. The inflow argon gas has a uniform velocity of 400m/s, a temperature of 60K, and a number density of $10^{24}/m^3$. Values of several

parameters used in the developed kinetic model are set as follows: $C_n = 10^{28}$, $q_s = 1.0$, $C_a = 2.0$, and $C_b = 1.175$.

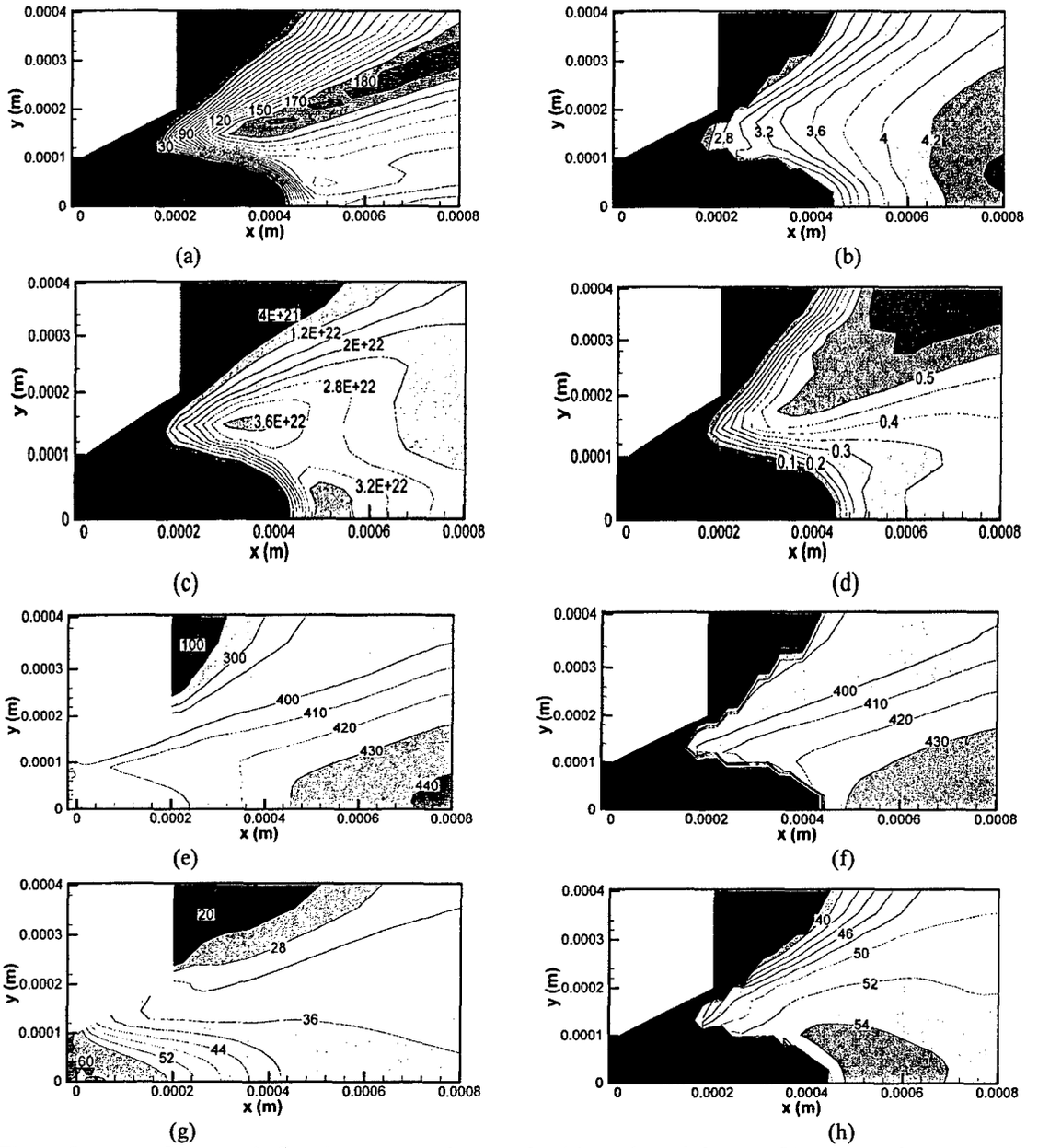

Figure 5. Supersonic flow in an expansion nozzle. *(a) number of clusters, (b) average cluster size, (c) number density of clusters ($1/m^3$), (d) mass fraction of clusters, (e) gas velocity (m/s), (f) cluster velocity (m/s), (g) gas temperature (K), (h) cluster temperature (K).*

The flow patterns of this problem are illustrated in Fig. 5. Figure 5(a) shows the number of clusters formed in the simulated domain (the average particle number in each cell is about 500). Clearly, the clusters are formed in a relatively small region (Fig. 5(c)), and the cluster size increases as the clusters move downstream in the flow (Fig. 5(b)). So the mass fraction of clusters also increases downstream the flow (Fig. 5(d)). It is found that the velocity of clusters (Fig. 5(f)) is very close to the gas velocity (Fig. 5(e)), whereas the cluster temperature (Fig. 5(h)) is larger than the gas temperature (Fig. 5(g)) because there are few reflection collisions between gas molecules and clusters. If we decrease the sticking coefficient, then few gas molecules will condense onto each cluster (Fig. 6(b)). However, there are more clusters formed in the flow (Fig. 6(a)). The temperature of both gas and cluster decreases, and the difference between them also decreases. If we decrease the nucleation rate ($C_n = 10^{22}$), then clusters are formed further downstream of the nozzle (Fig. 7(a)) where the degree of

supersaturation is larger. The average size of clusters increases, and the temperature of both gas and clusters decreases as expected.

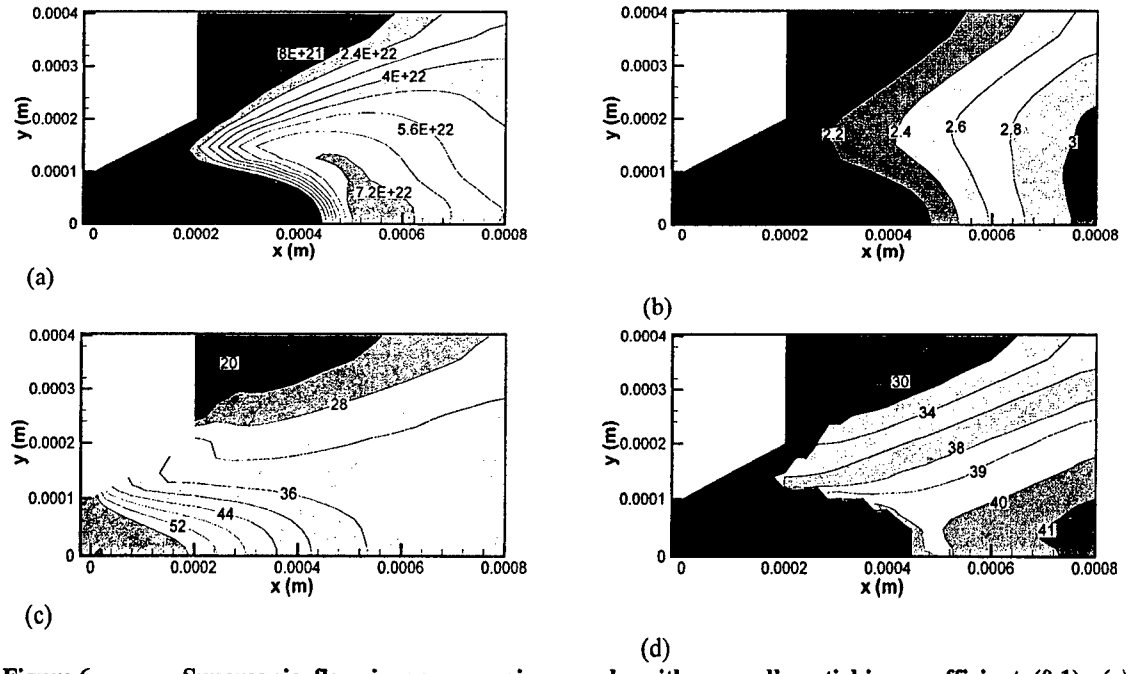

Figure 6. **Supersonic flow in an expansion nozzle with a smaller sticking coefficient (0.1).** *(a) number of clusters, (b) average cluster size, (c) gas temperature (K), (d) cluster temperature(K).*

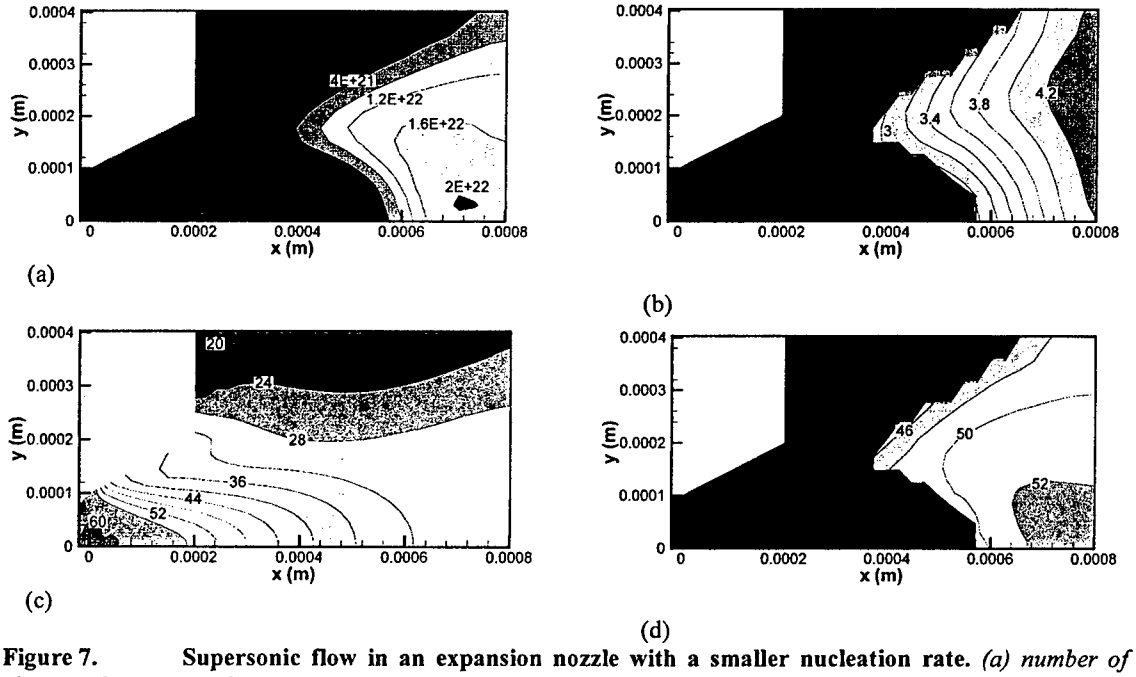

Figure 7. **Supersonic flow in an expansion nozzle with a smaller nucleation rate.** *(a) number of clusters, (b) average cluster size, (c) gas temperature (K), (d) cluster temperature (K).*

Discussion and Conclusion

Gas nucleation and condensation is very common in both nature and industry. There have been many studies on this topic. The classical nucleation theory is able to explain some physics of the nucleation processes, and

molecular dynamics simulation is supposed to expose the detailed mechanism of gas nucleation and condensation. However, due to the physical inaccuracy of the classical nucleation theory for small clusters and the extremely expensive numerical cost for molecular dynamics simulations, there is no general tool for studying gas flows having clusters.

The direct simulation Monte Carlo method is a less numerically expensive but still kinetically accurate method. We develop a general nucleation and condensation model and implemented it in the DSMC method, and thus detailed flow simulation becomes possible for flows involving clusters. In this model, clusters are modeled as particles, but both internal energy and potential energy are considered. Gas nucleation and condensation are modeled via particle collisions. The probability for possible nucleation or condensation, however, cannot be determined from the model itself. Since there are many uncertainties in the physics of nucleation and condensation, the DSMC method is very useful to investigate effects of parameters on general flow properties.

Our parametric studies showed that the proposed model was able to test effects of different parameters. The nucleation rate affected not only the number of clusters and cluster size but also the properties of the remaining gas. Investigation also showed that the sticking coefficient was very important for both cluster and gas properties. The application of the proposed model to a model example, supersonic flow in an expansion nozzle, demonstrated the capability of the proposed model: it is able to simulate complicated flows involving clusters and can predict detailed flow properties of both gas and clusters.

References

[1]Zhang, R, et al., "Atmospheric New Particle Formation Enhanced by Organic Acids," *Science*, Vol. 304(5676), 2004, pp. 1487-1490.

[2]Urban, D.L., and Faeth, G.M., "Soot Research in Combustion Science: Introduction and Review of Current Work," AIAA 2001-0322, 2001.

[3]Wu, B.J., "Possible Water Vapor Condensation in Rocket Exhaust Plumes," *AIAA Journal*, Vol. 13(6), 1975, pp. 797-802.

[4]Hill, P.G., "Condensation of Water Vapour During Supersonic Expansion in Nozzles," *Journal of Fluid Mechanics*, Vol. 25(3), 1966, pp. 593-620.

[5]McIlroy, D.N., et al., "Nanoparticle Formation in Microchannel Glass by Plasma Enchanced Chemical Vapor Deposition," *Journal of Applied Physics*, Vol. 93(9), 2003, pp. 5643-5649.

[6]Selwyn, G.S., Singh, J., and Bennette, R.S., "Insitu Laser Diagnostic Studies of Plasma-Generated Particulate Contamination," *Journal of Vacuum Science & Technology A*, Vol. 7(4), 1989, pp. 2758-2765.

[7]Liu. S., Xie, E., Sun, J., Ning, C., and Jiang, Y., "Astudy on Nano-Nucleation and Interface of Diamond Film Prepared by Hot Filament Assisted with Radio Frequency Plasma," *Materials Letters*, Vol. 57(11), 2003, pp. 1662-1669.

[8]Abraham, F. F., *Homogeneous Nucleation Theory*, Academic Press, 1974.

[9]Oxtoby, D. W., "Homogeneous Nucleation: Theory and Experiment," *Journal of Physics: Condensed Matter*, Vol. 4, 1992, pp. 7627-7650.

[10]Lothe, J., and Pound, G.M., "Reconsiderations of Nucleation Theory," *Journal of Chemical Physics*, Vol. 36(8), 1962, pp. 2080-2085.

[11]Hettema, H., and McFeaters, J. S., "The Direct Monte Carlo Method Applied to the Homogeneous Nucleation Problem," *Journal of Chemical Physics*, Vol. 105 (7), 1996, pp. 2816-2827.

[12]Toxvaerd, S., "Molecular Dynamics Simulations of Nucleation," *Molecular Simulation*, Vol. 30(2-3), 2004, pp. 179-182.

[13]Zurek, W.H., and Schieve, W.C., "Molecular Dynamics Study of Clustering. I," *Journal of Chemical Physics*, Vol. 68(3), 1978, pp. 840-846.

[14]Weiss, S., "Dimer and Trimer Formation in Dense Gaseous Argon: A MD Study," *Journal of Physical Chemistry A*, Vol. 101(18), 1997, pp. 3367-3370.

[15]Soto, R., and Cordero, P., "Cluster Birth-Death Processes in a Vapor at Equilibrium," *Journal of Chemical Physics*, Vol. 110(15), 1999, pp. 7316-7325.

[16]Toxvaerd, S., "Molecular Dynamics Simulations of Nucleation," *Molecular Simulation,* Vol. 30(2-3), 2004, pp. 179-182.

[17]Bird, G. A., *Molecular Gas Dynamics and the Direct Simulation of Gas Flows*, Oxford University Press, 1994.

[18]Briehl, B., and Urbassek, H. M., "Monte Carlo Simulation of Growth and Decay Processes in a Cluster Aggregation Source," *Journal of Vacuum Science and Technology A*, Vol. 17(1), 1999, pp. 256-265.

[19]Mizuseki, H, Jin, Y., Kawazoe, Y., and Wille, L.T., "Growth Processes of Magnetic Clusters Studied by Direct Simulation Monte Carlo Method," *Journal of Applied Physics*, Vol. 87(9), 2000, pp. 6561-6563.

[20]Insepov, Z., and Yamada, I., "Direct Simulation Monte Carlo Method for Gas Cluster Ion Beam Technology", *Nuclear Instruments and Methods in Physics Research B*, Vol. 202, 2003, pp. 283-288.

[21]Zhong J., Gimelshein S. F., Zeifman, M. I., and Levin, D. A., "Modeling of Homogeneous Condensation in Supersonic Plumes with the DSMC Method," AIAA 2004-0166, 2004.
[22]Sun, Q., Boyd, I.D., and Tatum, K.E., "Particle Simulation of Gas Expansion and Condensation in Supersonic Jets," AIAA 2004-2587, 2004.
[23]Perrell, E. R., Erickson, W. D., and Candler, G. V., "Numerical Simulation of Nonequilibrium Condensation in a Hypersonic Wind Tunnel," *Journal of Thermophysics and Heat Transfer*, Vol. 10(2), 1996, pp. 277-283.
[24]Itkin, A.L., "Kinetic Model of Coupled Nonequilibrium Condensation and Radiative Excitation of Water Molecules," *Journal of Chemical Physics*, Vol. 108(9), 1998, pp. 3660-3677.
[25]Hillenkamp, M., Keinan, S., and Even, U., "Condensation Limited Cooling in Supersonic Expansions," *Journal of Chemical Physics*, Vol. 118(19), 2003, pp. 8699-8705.
[26]Zeifman, M.I., Zhong, J., and Levin, D.A., "A Hybrid MD-DSMC Approach to Direct Simulation of Condensation in Supersonic Jets," AIAA 2004-2586, 2005.
[27]Zhong, J, Zeifman, M.I., and Levin, D.A., "A Kinetic Model of Condensation in a Free Argon Expanding Jet," AIAA 2005-767, 2005.
[28]Dietrich, S., and Boyd, I.D., "Scalar and Parallel Optimized Implementation of the Direct Simulation Monte Carlo Method," *Journal of Computational Physics*, Vol. 126, 1996, pp. 328-342.
[29]Sun, Q., and Boyd, I.D., "Evaluation of Macroscopic Properties in the Direct Simulation Monte Carlo Method," *Journal of Thermophysics and Heat Transfer* (to be published).
[30]Hale, B.N., "Monte Carlo Calculations of Effective Surface Tension for Small Clusters," Austrian *Journal of Physics*, Vol. 49, 1996, pp. 425-434.

2. 12V Flow Investigations

HALL thrusters represent an efficient form of plasma electric propulsion for spacecraft. They offer a high specific impulse that is well suited for satellite station-keeping, repositioning, and orbit transfer. There are concerns, however, about the plumes. For instance, the plumes may contaminate spacecraft surfaces and interfere with satellite communications. Such effects need to be understood during the development of thrusters and their integration onto spacecraft. Successful integration of plasma thrusters onto spacecraft involves a mixture of analysis and ground-based experiments conducted in vacuum chambers. A key aspect of the vacuum chamber experiments is the desire to maintain as low a back pressure as possible. Elevated back pressures can lead to augmentation of thrust and distortion of the plasma plume, thereby complicating the process of integration assessment. The 12V vacuum chamber located at the Arnold Engineering Development Center (AEDC) is a large facility with a total pumping rate of about $3\text{-}5\text{x}10^6$ litres/sec on xenon. For thruster mass flow rates of 10-20 mg/sec, it is able to maintain a back pressure on the order of 10^{-6} torr. Further details of the facility and its operation can be found in Ref. 1. In addition to providing a physical test capability, AEDC has a desire to provide computational analysis support for customers interested in using their facilities. The focus of the present work is on the development of an analysis tool that can be applied at AEDC to model the operation of different plasma thrusters in the 12V vacuum chamber. The present study is limited to investigation of Hall thruster plumes.

In general, the near plume of a Hall thruster consists of neutrals, highly energetic ions, and electrons. The particles have collisions due to their thermal velocities, and some collisions between neutrals and ions lead to charge-exchange interactions, which produce slow ions and highly energetic neutrals. Furthermore, the ions are also affected by the self-consistent electric fields. In addition, a background gas is always involved in the ground tests of thrusters. Therefore, the behavior of thruster plumes is very complicated. An efficient approach for understanding these processes is to use computer modeling[2] because the physics at different levels can be included for the plume. For instance, the direct simulation Monte Carlo (DSMC) method[3] can be used to capture the collision dynamics, and the particle-in-cell (PIC) method[4] can be applied to include the electric field effects. In addition, computer simulations can identify the relative importance of the physics involved in the plume.

In this paper, particle simulation of a Hall thruster plume in 12V is investigated using a hybrid DSMC/PIC code. The rest of the paper is organized as follows. Section II introduces the numerical method. Section III describes the plume simulation. Section IV investigates effects of different physics and compares simulation results and measurement data. Finally, some concluding remarks are given in Section V.

Numerical Method

Hall thrusters primarily use xenon as propellant. The plume is comprised of beam ions with velocities on the order of 20 km/s, low energy charge-exchange ions, neutral atoms from the thruster, electrons, and the background gas of the experimental facility. The interactions of these species as well as the influence of the

electric fields are the important modeling issues. Computational analysis of Hall thruster plumes is regularly performed using a hybrid particle-fluid formulation. The direct simulation Monte Carlo (DSMC) method models the collisions of the heavy particles (ions and neutrals). The particle-in-cell (PIC) method models the transport of ions in electric fields.

Collision Dynamics

The DSMC method uses particles to simulate collision effects in rarefied gas flows. The particles represent real ions and neutrals, and are grouped in cells whose sizes are less than a mean free path. Pairs of these particles are selected at random and a collision probability is evaluated that is proportional to the product of the relative velocity and collision cross section for each pair. The probability is then compared with a random number between zero and one to determine if that collision occurs. If so, some form of collision dynamics is performed to alter the properties of the colliding particles.

There are two types of collisions that are important in the Hall thruster plume: elastic (momentum exchange) and charge exchange. Elastic collisions involve only exchange of momentum between the participating particles. For the systems of interest here, this may involve neutral-neutral or neutral-ion collisions. For neutral-neutral collisions, the variable hard sphere collision model[3] is employed. The collision cross section for xenon is:

$$\sigma_{EL}(Xe, Xe) = \frac{2.12 \times 10^{-18}}{g^{2\omega}} m^2 \tag{1}$$

where g is the relative velocity and $\omega = 0.12$ is related to the viscosity temperature exponent for xenon. For neutral-ion elastic interactions, the following cross sections measured by Miller et al.[5] are employed:

$$\sigma_{EL}(Xe, Xe^{+}) = (175.26 - 27.2 \log_{10}(g)) \times 10^{-20} m^2 \tag{2}$$

$$\sigma_{EL}(Xe, Xe^{++}) = (103.26 - 17.8 \log_{10}(g)) \times 10^{-20} m^2 \tag{3}$$

Charge exchange concerns the transfer of one or more electrons between an atom and an ion. The cross sections are assumed to follow the same expressions for neutral-ion elastic collisions. In the present model, it is assumed that there is no transfer of momentum accompanying the transfer of the electron(s). This assumption is based on the premise that charge exchange interactions are primarily at long range.

Plasma Dynamics

The PIC algorithm uses charged particles and determines the charge density at the nodes of the mesh, based on the proximity of each particle to the surrounding nodes. The charge density is then used to calculate the potential at the nodes. The plasma potential can be described using the Boltzmann relationship that is derived by keeping only the dominant terms of the electron momentum equation and assuming isothermal electrons:

$$\phi - \phi_{ref} = \frac{kT_e}{e} \ln\left(\frac{n_e}{n_{ref}}\right) \tag{3}$$

The potential is then differentiated spatially to obtain the electric fields that are used to transport the ions.

Boundary Conditions

For the computations of the Hall thruster plume in 12V, boundary conditions must be specified at the thruster exit and along all solid surfaces in the computational domain.

Several macroscopic properties of the plasma exiting the thruster are required for the computations. Specifically, the plasma potential, the electron temperature, and for each species the number density, velocity, and temperature are required. These properties are determined using an approach involving a mixture of analysis and estimation.[5] Several types of surfaces are included in the computation. They are thruster walls, cryopump surfaces, baffles, and chamber walls. Along these walls, the plasma potential is set to zero. Any ions colliding with the walls are neutralized. When particles hit the cryopump surfaces, a fraction of the particles are pumped away, which is characterized by a sticking coefficient (a value of 0.8 is used in the present study). For

particles scattered back into the flow field from all surfaces, a diffuse reflection is assumed characterized by the surface temperature.

Plume Simulation

The 12V chamber at AEDC is an Electric Propulsion (EP) test facility, whose height is about 12 m. The chamber has a relatively complex axi-symmetric geometry. As shown in Fig. 1, the thruster is mounted on the chamber axis and fired downward. There are three baffles in the "waist" area and three more near the center of the chamber bottom. Two cryopumps are employed to pump the plume away. In the present study, the plume is generated by a 4.5 kW class xenon Hall thruster (the Aerojet BPT-4000). If the vacuum chamber is assumed empty when the thruster starts to fire, simulation (Fig. 2) shows that it will take about 1 second to balance the mass in the plume due

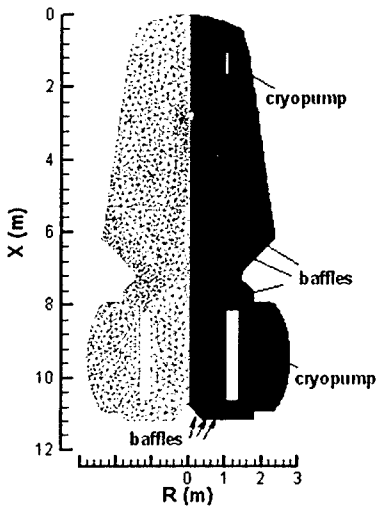

Figure 1. Mesh for the 12V chamber.

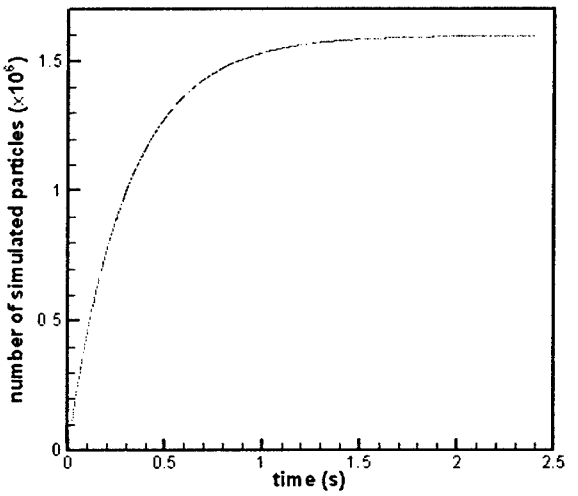

Figure 2. Approach to steady state in the simulation

to the thruster firing and the pumping. There is one main reason for taking a long time to reach a steady state for this high-speed plume. The cryopump panels are at very low temperature (20K) so that the thermal velocity of particles reflected from the panels is very small, which indicates that the characteristic speed of background particles (reflected neutrals) is about one order of magnitude smaller than the neutral velocity in the near plume and three orders of magnitude smaller than the ion velocity in the nozzle exit.

The relatively large speed at the thruster exit establishes a near field plume in a very short time whereas the far field plume requires a much longer time, which can be illustrated by showing the total number density at two different times (Fig. 3). The ions establish themselves much more rapidly as indicated by the relatively minor changes observed in Fig. 4 for these two times. The more rapid convergence of the plasma component is further illustrated in Fig. 5 that shows the behavior of plasma potential. The different behavior of neutrals and ions is also illustrated in Fig. 6 by showing the streamlines of the individual species. Specifically, the ions are emitted from the thruster exit and are lost on any surfaces, whereas the neutrals come from both the thruster exit and the surfaces of baffle and chamber, and are only removed by the cryopumps.

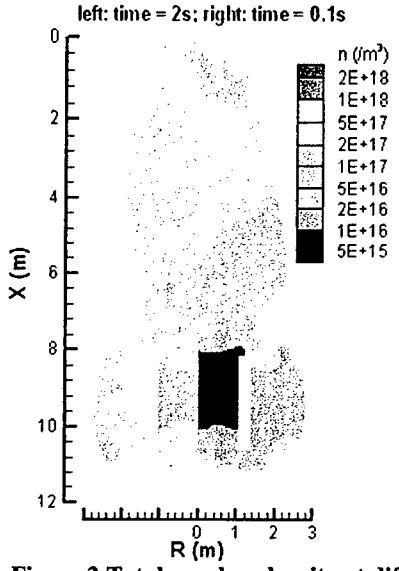

Figure 3.Total number density at different times.

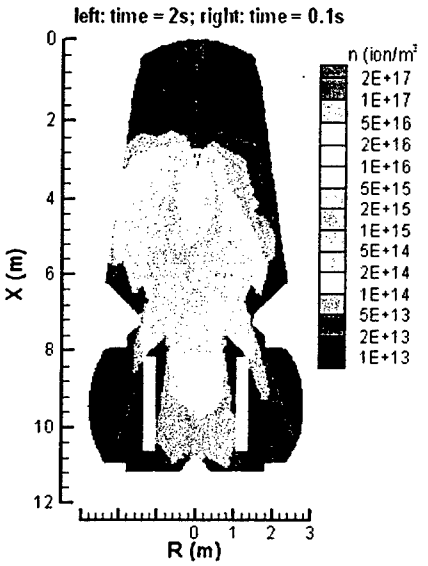

Figure 4. Ion number density at different times.

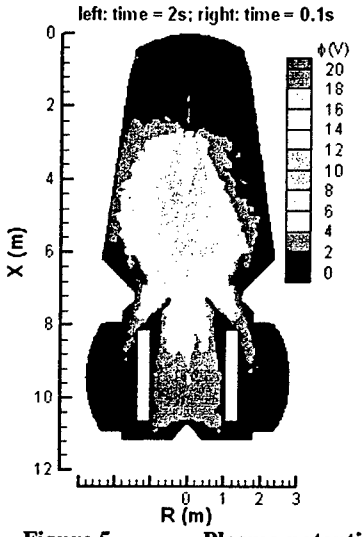

Figure 5. Plasma potential at different times.

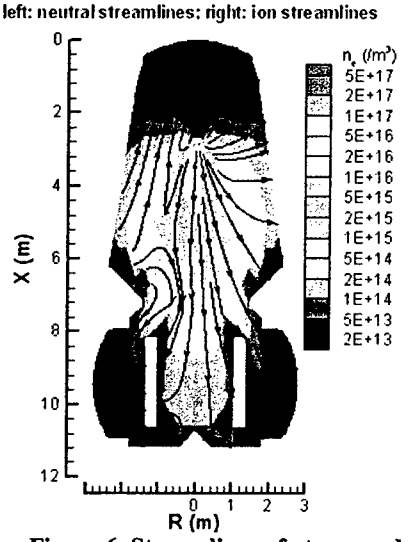

Figure 6. Streamlines of atoms and ions.

Physics Modeling

A series of plume simulations are conducted to quantify the effects of different physical mechanisms on the plasma plume structure. Specifically, three simulations are performed: (1) with charge exchange and electro-static fields (DSMC, PIC, CEX); (2) with electro-static fields and no charge exchange (DSMC, PIC), and (3) with charge exchange and no electro-static fields (DSMC, CEX). Results from these simulations are compared in Figs. 7a and 7b for the total number density. In Fig. 7a, the full simulation result is shown on the left, and the simulation omitting charge exchange and including electro-static fields is shown on the right. In Fig. 7b, the right hand solution includes charge exchange collisions but now omits the electric fields. There are relatively minor differences between these three solution results indicating that the overall pressure distribution in the 12V chamber is largely unaffected by the additional physics. The same comparisons are made in Figs. 8a and 8b for the plasma density. Figure 8a indicates that charge exchange has a relatively weak effect on the plasma distribution except for the backflow region behind the thruster. By contrast, Fig. 8b shows that omitting the electric fields creates a significantly different plasma plume structure

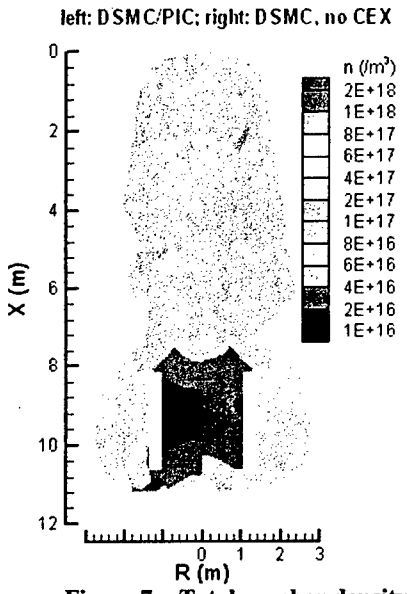

Figure 7a. Total number density obtained with different physical models.

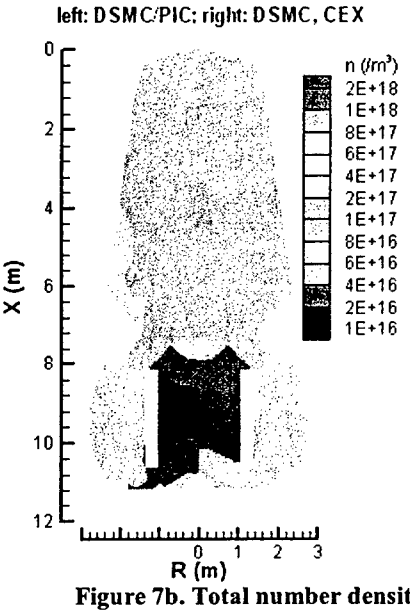

Figure 7b. Total number density obtained with different physical models.

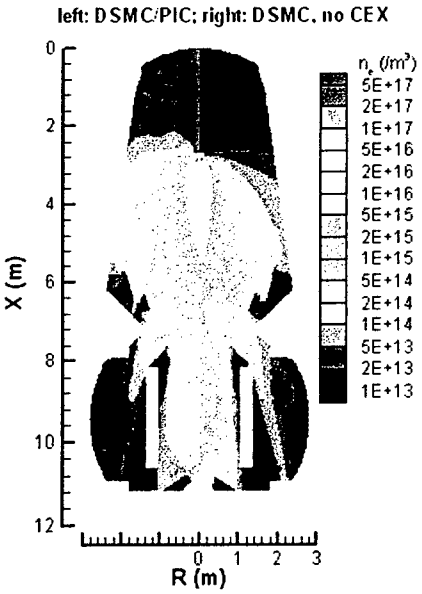

Figure 8a. Plasma number density obtained with different physical models.

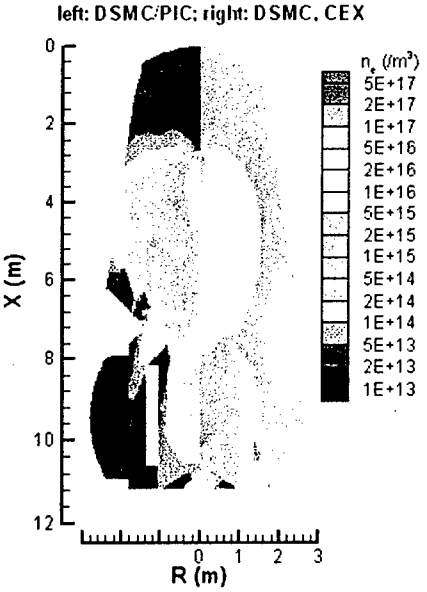

Figure 8b. Plasma number density obtained with different physical models.

Comparison is also made between the simulation results and measurement data. In Ref. 7, the application is reported of a microwave interferometry diagnostic for measurement of plasma density in 12V in the plume of the BPT-4000 Hall thruster. Raw data and best curve fits are presented in Ref. 7 of the plasma density distributions. In our use of these data sets, the error bar is set as 50% of the curve fitted value based on our observations of the effectiveness of the curve fit. In Fig. 9a, comparisons between the three different simulations are shown for the radial plasma density profiles at five different axial distances from the thruster exit plane. These profiles show quantitatively the same trends illustrated in Figs. 7-8. Namely, that omitting the electric fields has a much greater effect on the plume structure than omitting the charge exchange collisions. In Fig. 9b, the full DSMC/PIC simulation results (including both charge exchange and electric fields) are compared with the curve-fits provided by Meyer et al.[7] The simulation and measurement profiles are in

remarkably good agreement at all locations in the plume considered The two data sets lie within the uncertainty level of the curve-fit data at all points. For reference, Fig. 9c is taken directly from Ref. 7 and compares the curve fits with the raw measurement data. Comparison of the raw measurement data in Fig. 9c with the DSMC/PIC results in Fig. 9b shows even better agreement than with the curve-fit data. The excellent levels of agreement obtained in these comparisons serves as a strong validation of the DSMC-PIC code developed for analysis of plasma plumes in the 12V facility.

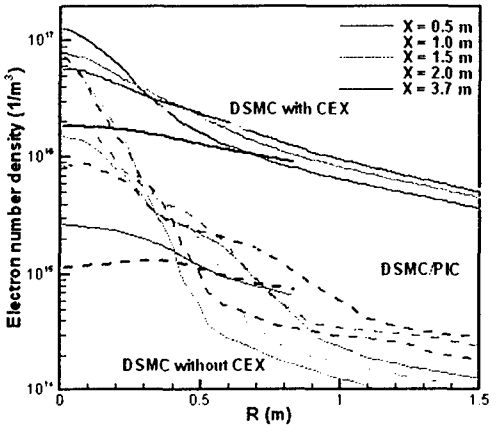

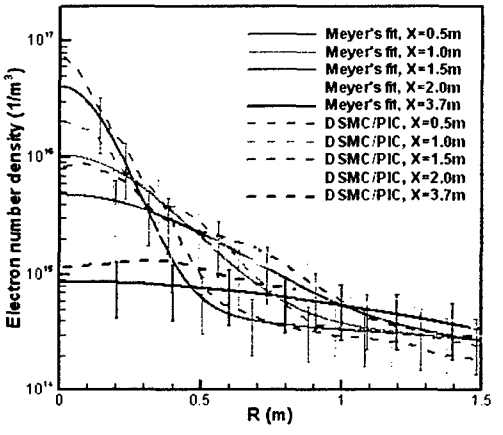

Figure 9a. Radial Profiles of plasma number density Figure 9b. Radial Profiles of plasma number density

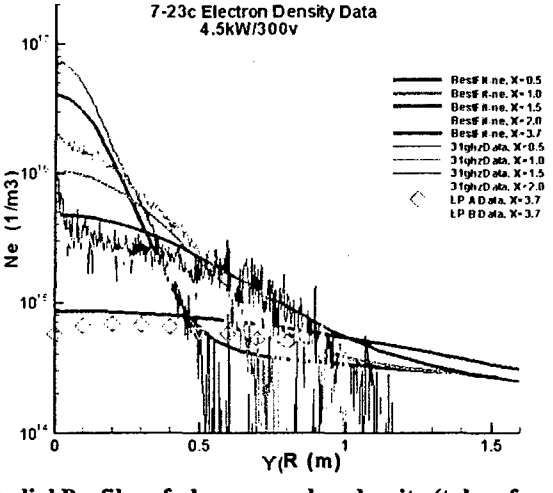

Figure 9c. Radial Profiles of plasma number density (taken from Ref. 7).

Conclusions

A general purpose, hybrid DSMC-PIC-fluid code has been developed for simulation of plasma plumes from thrusters operated in the 12V electric propulsion facility at AEDC. The code was applied to model the plasma plume structure from the BPT-4000 Hall thruster. A series of simulations was performed in order to assess the sensitivity of the computed results to inclusion of different levels of physical modeling fidelity. Comparison of these results indicated that the electric fields have a significantly stronger impact on the plasma plume structure than charge exchange collisions. The physical accuracy of the full plume simulation was assessed through comparisons of previous measurements of plasma number density in the thruster plume obtained with a microwave interferometer. Excellent agreement was obtained between simulation and measurement for all plume locations considered. The simulation tool is therefore considered validated for application to this class of Hall thruster.

References

[1]Pruitt, D., Dawbarn, A., Bauer, M., et al., "Development of a Novel Electric Propulsion Test and Evaluation Capability at AEDC," AIAA 2002-4338, July 2002.

[2]Boyd, I. D., "Review of Hall thruster plume modeling," *Journal of Spacecraft and Rockets*, Vol. 38, No. 3, 2001, pp. 381-387.

[3]Bird, G. A., *Molecular Gas Dynamics and the Direct Simulation of Gas Flows*, Clarendon Press, 1994.

[4]Birdsall, C. K., and Langdon, A. B., *Plasma Physics via Computer Simulation*, Adam Hilger, U.K., 1991.

[5]Miller, J. S., Pullins, S. H., Levandier, D. J., Chiu, Y., and Dressler, R. A., "Xenon charge exchange cross sections for electrostatic thruster models," *Journal of Applied Physics*, Vol 91, No. 3, 2002, pp. 984-991.

[6]Boyd, I. D. and Yim, J. T., "Modeling of the near field plume of a Hall thruster," Journal of Applied Physics, Vol. 95, No. 9, 2004, pp. 4575-4584.

[7]Meyer, J. W., Loane, J. T., Hallock, G. A., Wiley, J. C., and Dawbarn, R. A., "Hall Thruster Plume signal Transmission Testing in the AEDC 12V Vacuum Chamber," AIAA 2005-4049, July 2005.